Developing Atomic Layer Deposition Techniques of Tungsten on Carbon Nanotube Microstructures

Jason Kyle Anderson

A senior thesis submitted to the faculty of
Brigham Young University
in partial fulfillment of the requirements for the degree of

Bachelor of Science

David Allred, Advisor

Department of Physics and Astronomy

Brigham Young University

April 2014

ABSTRACT

Developing Atomic Layer Deposition Techniques of Tungsten on
Carbon Nanotube Microstructures

Jason Kyle Anderson
Department of Physics and Astronomy
Bachelor of Science

Traditional microfabrication processes are confined to a small set of materials due to limitations on etching and confined to low-aspect-ratio fabrication due to limits in both etching and stability of thicker film deposition processes. Carbon Nanotube Templated Microfabrication (CNT-M) technology has introduced a dramatically different approach to microfabrication that fabricates without significant etch processes. This is achieved by forming the desired structure in carbon nanotubes (CNT) and then filling or infiltrating that structure with the material of choice. This technology has been developed at BYU using materials like silicon and carbon. Microfabrication with metals is needed because of their higher density and improved electrical and mechanical properties compared to traditional microfabrication materials. A suitable metals process has not yet been found. We endeavored to develop atomic layer deposition (ALD) of W using atomic H as the agent for abstracting the nonmetal atoms such as C, O or F that act as ligands for the gaseous form of W used to bring the W into the deposition. We used tungsten hexafluoride (WF_6) and molecular hydrogen as our reactants, flowing them in alternating cycles onto carbon nanotube samples in a vacuum chamber. We did not achieve significant W deposition in the initial process, so we incorporated a microwave generator to replace the H_2 with hydrogen plasma. This somewhat improved deposition, but an even bigger improvement in deposition came when the samples were ozone treated before deposition. This process achieved a final product composed of 60% W as measured using and EDAX system in an SEM. This deposition was still too limited to allow for mechanical and electrical tests of the samples, which were too fragile for liftoff from the substrate.

Keywords: [A comma-separated list of descriptive words for search purposes]

ACKNOWLEDGMENTS

I would like to first thank Dr. David Allred, my research advisor, who helped me come up with the idea for this project. He suggested this idea to me, and has been very helpful in getting it accomplished. His advice, and that of the other professors in our research group, Robert Davis and Richard Vanfleet, was crucial in moving this project along when we were stuck. I would like to thanks Lawrence Reese for his help in training me to use specific systems. Lastly, I would like to thank Collin Brown, who has helped me to tag-team this project. I would not have gotten as far along as I did without his help.

Contents

List of Figures

Chapter 1

Introduction

1.1 Traditional Microfabrication Processes

Microfabrication is the creation of structures on a micro meter scale. These structures are traditionally used for integrated circuits or microelectromechanical systems (MEMS). Microfabrication of metals is sought after for their higher density, and improved electrical and mechanical properties as compared to silicon and other traditional micro fabrication materials. This fabrication is traditionally done by an etching process, whether mechanical or chemical, and matter is removed from a material in order to achieve the desired shape. Chemical etching is able to achieve better definition of features than mechanical etching, however, it is restricted in two ways. The first is that chemical etching is limited to a small subset of possible materials to create features from due to necessary chemical interactions. This limits the materials that you can use to create MEMS. The second limitation is that features created with chemical etching are not able to achieve a high aspect ratio. The aspect ratio is the height of a feature compared to its width, and a high aspect ratio is desirable in MEMS so that you can get relatively tall features that are none-the-less well defined. The reason for the aspect ratio limit in chemical etching is a physical one.

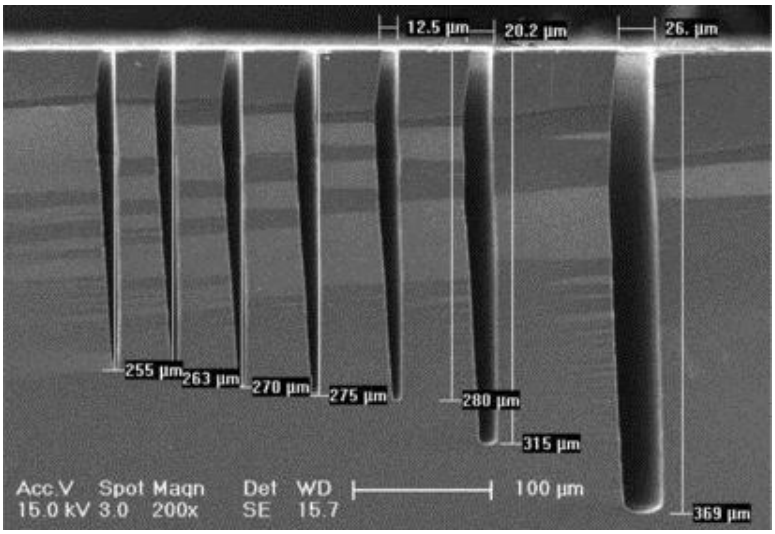

Figure 1.1 A cross sectional view of RIE lag on a silicon base.

When etching very thin tunnels into a feature, transportation of reactant gas from the chemical gas upwards hinders the downward progress of the reactive agent. This effect is also seen in reactive ion etching (RIE) processes, and is known as RIE lag [1]. Fig. 1.1 shows the effects of RIE lag, as the etching effectiveness is clearly decreased as the channel width decreases. In order to avoid uneven etching depths, a low aspect ratio has to be maintained in feature design. In an attempt to avoid these limitations on aspect ratio, researchers at BYU are developing a new fabrication technique called Carbon Nanotube Templated Microfabrication.

1.2 Carbon Nanotube Templated Microfabrication

Carbon nanotube templated microfabrication (CNT-M) technology has introduced a dramatically different approach to microfabrication that is able to fabricate microstructures without relying on significant etching processes. This is achieved by forming the desired structure out of carbon nanotubes and then filling, or infiltrating, that structure with the material of choice through deposition techniques. CNT make a very good medium because of the degree of precision achievable. Car-

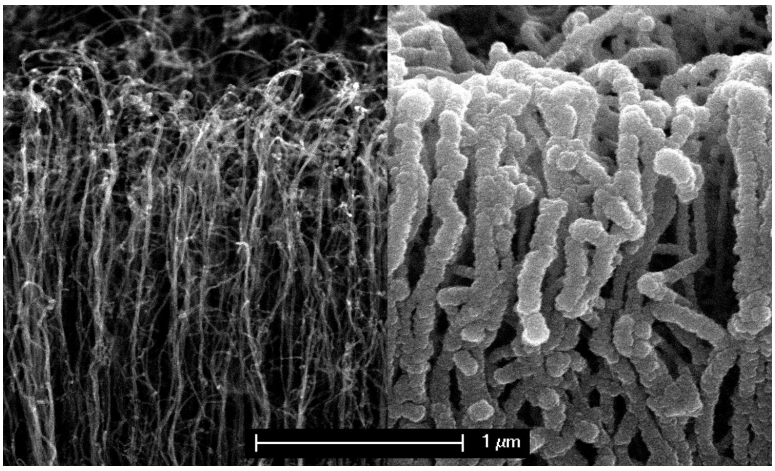

Figure 1.2 A view of individual carbon nanotubes on the left and ones that have been infiltrated with MO(CO)6 by Richard Hansen.

bon nanotube structures can have an aspect ratio upwards of 2:1 [2]. The physical composition of the carbon allotrope comprising nanotubes allows the carbon structures to be conductive as well, which is beneficial towards our end-goal of creating MEMS. Carbon nanotubes are also ideal for infiltration because of their low density. Less than one percent of carbon nanotube forests is actually carbon, the rest is vacant space which can be filled with your desired element. Figure 1.2 shows the available space in an uninfiltrated forest versus one that has been infiltrated. Ideally this infiltration can lead to a solid structure of your ideal element that has been shaped by the design of the nanotube forest. This microfabrication process has been developed at BYU using materials like silicon and carbon; however, a suitable metals process has not yet been found [3].

Attempts were made at Brigham Young University by David McKenna and Richard Hansen to infiltrate carbon nanotube forests using Chemical Vapor Deposition (CVD) Techniques [4] [2]. The process for CVD is to heat up your sample and your infiltrating element inside a vacuum and use an inert gas to blow the element directly onto the forest. The CVD method yielded deposition of molybdenum onto a nanotube forest, but the process was largely plagued with element buildup on the edges that prevented further infiltration of the structure [2].

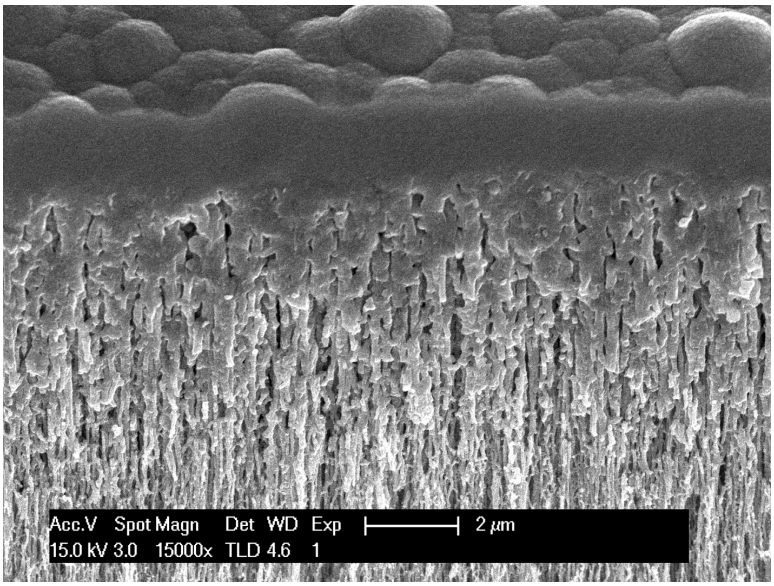

Figure 1.3 A cross-section of the capping layer formed on a nanotube forest. This forest has been infiltrated with MO(CO)6 by Richard Hansen.

This problem is known as capping. Figure 1.3 shows a cross-sectional view of outer capping and limited internal deposition from CVD techniques. In order to avoid this problem we decided to try an alternative technique called ALD.

1.3 Atomic Layer Deposition

Atomic Layer Deposition (ALD) is a technique of infiltration that tries to avoid the problem of capping by limiting deposition to small increments, theoretically as small a layer as one atom thick of your desired depositing agent. Because the deposition is so limited, the edges of the forest won't be clogged too quickly to prevent deep penetration of our gases. This gradual deposition is achieved through a multi-step chemical process and relies on the interaction of two gaseous reactants. The normal chemistry for ALD is to use a gaseous form of tungsten, tungsten hexafluoride (WF_6), and disilane (Si_2H_6).

The first step of ALD is to deposit WF_6 onto a nanotube forest. Because WF_6 is self-limiting,

the sample will theoretically have only one molecular layer thick deposition. The next step for ALD is to flow a reactant gas into the deposition chamber that will pull the fluorine off of the tungsten atoms. Disilane reacts very well with the fluorine, and the resulting gas is vented from the chamber, leaving the tungsten deposited on the structure one atom thick. This process is repeated through many cycles until one has achieved a uniform deposition throughout the forest to create a solid microstructure.

Researchers have shown some success with this process of deposition, so we decided that we would try to create a process of tungsten ALD using WF_6 and a hydrogen plasma. We predicted that the introduction of a hydrogen plasma to WF_6 would cause a reaction in which hydrofluoric (HF) gas is a product, as well as pure W. It was our goal to create high-density tungsten microstructures.

Chapter 2

Experimental Methods

2.1 Creating a Nanotube Forest

2.1.1 Substrate Preparation

The first step in creating a carbon nanotube forest is preparing a silicon substrate to grow the nanotubes on. This process of preparation begins with lithography. A silicon substrate with a top layer of SiO_2 is first coated with a photoresist layer which will react chemically when exposed to an electron beam lithograph. For our purposes we used AZ 3312 photoresist. The e-beam will have a specialized mask placed inside for a specific design so that only the desired parts of the photoresist are exposed. In our case we designed the mask to expose the areas of the substrate where we wanted nanotube growth to occur. After the photoresist has been exposed to the e-beam, the substrate is put into a chemical bath that will strip away the exposed areas, leaving uncoated areas in the photoresist in the pattern of the desired structure. We used Microposit 1165 to achieve this "liftoff".

Once the substrate has been patterned by lithography, the wafer is put into a thermal evaporator and about 6 nm of iron is deposited onto the structure [2]. Iron is deposited directly into the

uncoated areas in the shape of the desired structure, while the remaining parts of the substrate have a layer of photoresist between the iron layer and the SiO_2 layer. The substrate is then treated chemically treated to remove the final parts of photoresist, taking the iron layer with it. The final result of the lithography and iron deposition process is a silicon substrate with iron patterns in the shape of your desired structure. With inflowing hydrogen, this iron, which as reduced to iron oxide,will be the catalyst for nanotube growth in a furnace [5].

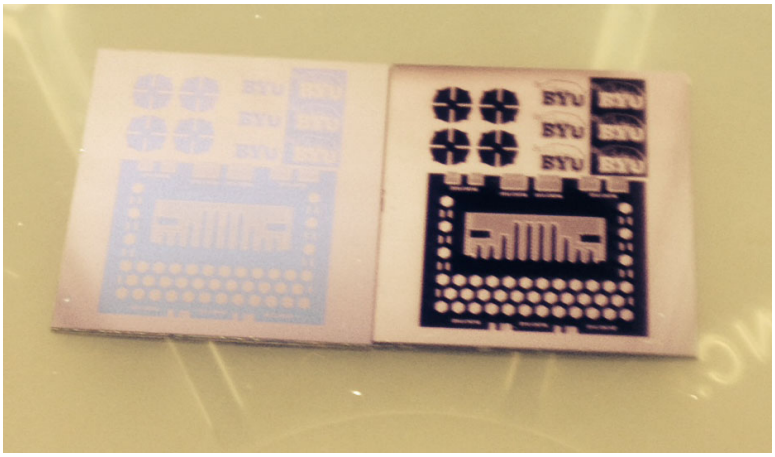

Figure 2.1 Two segments of a silicon wafer side by side. The sample on the left has gone through lithography and iron deposition. The sample on the right has carbon nanotubes grown on it.

2.1.2 Furnace Growth

The prepared sample is inserted into a furnace system which is raised to about 750° Celsius. This is done while flowing H_2 through the tube at 500 sccm. Once the furnace tube reaches 750°C, ethylene (C_2H_4) enters the chamber at 700 sccm. This ethylene contains the carbon that will form the nanotubes. Due to the high temperature, the iron deposits agglomerate into nanosized beads. The iron catalyzes the breakdown of the ethelyne. The carbon formed dissolves into the iron but also precipitates the build up of CNT. The result is that many tall tubes rise up from the substrate from the iron beads and form a forest of carbon nanotubes. The height of the forest is determined

by the length of time that ethylene is flown into the furnace chamber. Our samples were about 10-15μm in height, with an average exposure time of 10 seconds to the ethylene gas. These forests were then kept in sample holders to await tungsten deposition.

2.2 Structural Design

We specifically chose the designs of our samples to allow for eventual testing of the physical properties of the infiltrated tungsten structures. The sample design had multiple cantilever shapes that would be used to determine the flexibility and yield resistance of our structures. We also had van der Pauw disk shapes, a circular design that is used to determine electric resistivity of a material. By incorporating these shapes into our structure design, we allowed for electrical and mechanical characterization of our structures.

2.3 Converting a CVD System to ALD

2.3.1 Changes to the Schematics

The system we used was originally built as an ALD system, but was refurbished to accomodate CVD by David McKenna, a former researcher at BYU who worked extensively on microfabrication. Because of the original configuration, the system was compatible with our adaptations and did not require a complete overhaul. There were already multiple entry points for gases in the vacuum chamber, and the Labview program that controls the system had already incorporated the extra valves that would be needed to control two gases. We inserted a new line of stainless steel to transport the WF_6 directly to the chamber. We also added an additional line to create the hydrogen plasma. The hydrogen plasma was created by flowing molecular hydrogen (H_2) through a quartz tube that was surrounded by an antenna. The antenna was connected to a microwave generator

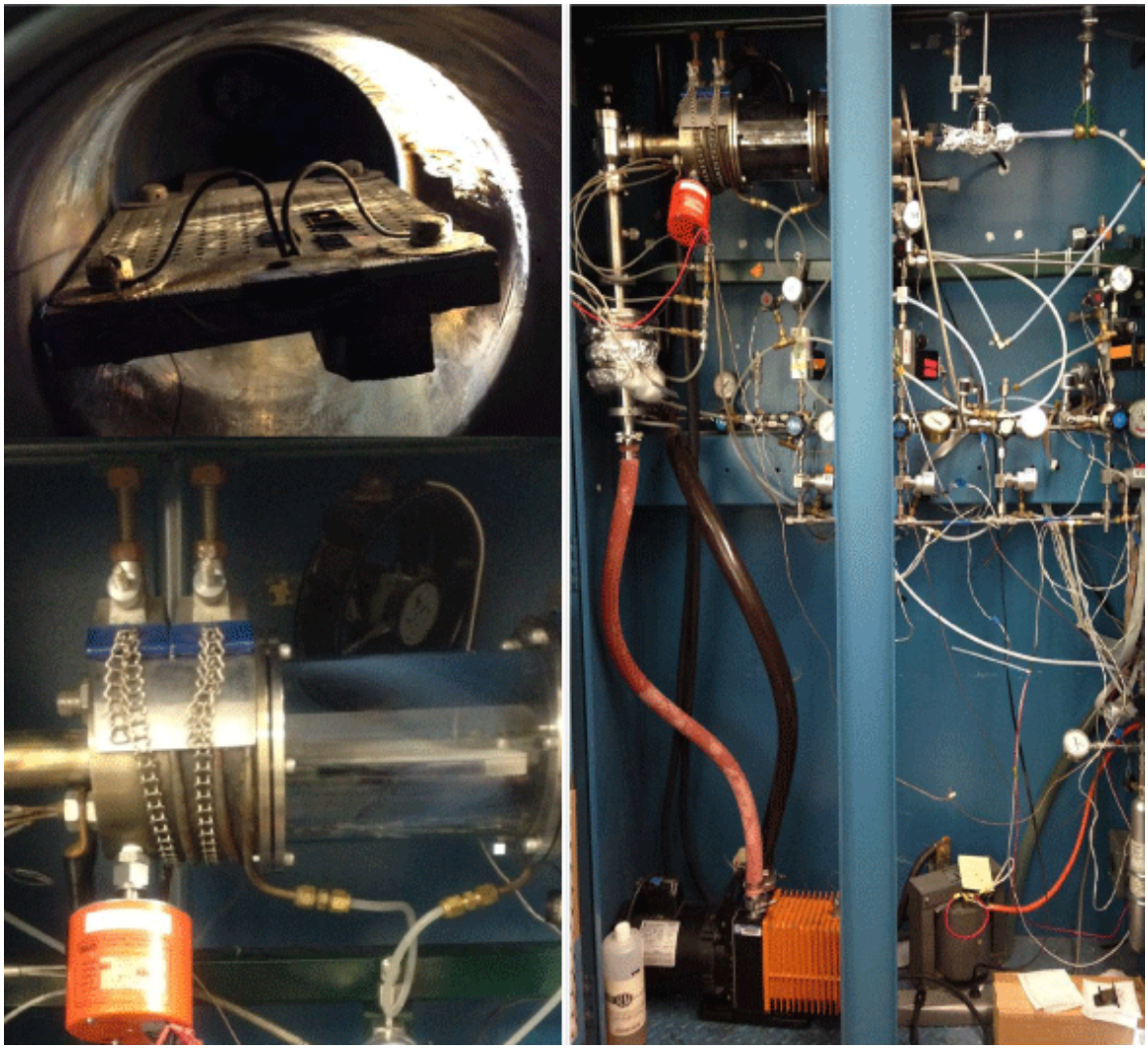

Figure 2.2 Top Left: The inside of the sample chamber. Bottom Left: The outside of the sample chamber. Right: A view of the whole ALD system.

which we used to excite the hydrogen gas into plasma. We drilled a hole into the gas cabinet that housed the system to allow for a cable between the generator and the antenna. We also created supports for the antenna by utilizing the Unistrut system that outlined the gas cabinet. This plasma then flowed into vacuum chamber using a new chamber cap that we created for this purpose.

We also added a bypass line between the plasma and the chamber to allow for continuous ignition of the hydrogen gas into plasma but also limit plasma exposure of the sample to well

controlled intervals. This was done to allow the WF_6 sufficient time to attach itself onto the CNT's.

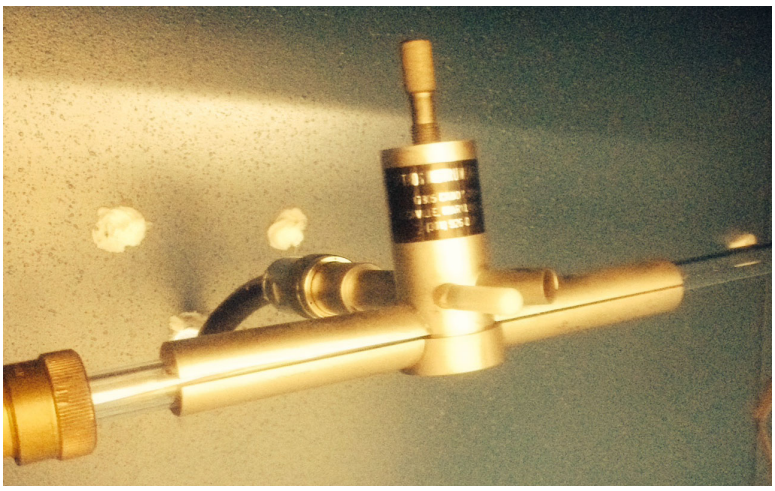

Figure 2.3 The antenna for the microwave generator clamped around a quartz tube.

2.3.2 Automating Labview

Because the pneumatic gas valves in the system were already hooked up electronically to the computer and recognized by Labview, the only thing we had to do was automate the control system. This was done by Collin Brown, a fellow researcher at BYU. The controllable features are flow rates, flow times, wait times, and cycle numbers.

2.3.3 Safety Precautions

Because the reduction is HF gas, we incorporated new safety features into the ALD system. We caulked all of the holes in the cabinet to prevent any gas which might leak from the lines or vacuum chamber from entering the lab. Between the WF_6 source and the steel lines we put an extra pneumatic valve so that we could control the amount of WF_6 gas entering the system. We also inserted new HF gas detectors into the exhaust system from the cabinet. These were incorporated into an existing alarm system for the lab. We also added a filtering chamber to the system between

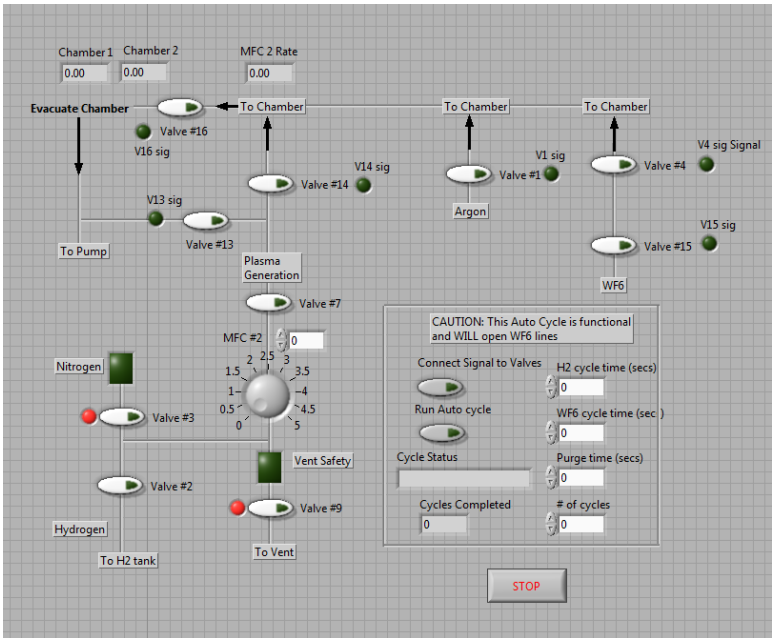

Figure 2.4 This shows the front control panel of the Labview control system. This was updated from the CVD control panel and automated by Collin Brown.

the sample chamber and the roughing pump we used to get the chamber down to vacuum. This filtering chamber was filled with steel wool and aluminum shavings which we heated to about 375°C. This was an effort to treat the HF gas before it entered the roughing pump and got into the pump oil. We have also incorporated an HF oil filter into the system to be used after repeated deposition runs.

2.4 Deposition Process

Typically, the first step in a deposition process is to insert the carbon nanotube sample into the sample chamber. This was placed directly on the chamber heater. The sample chamber was closed and we used a roughing pump to get the chamber down to about 400 millitorr. Because of periodic flow of gases into the chamber our pressure varied throughout the deposition process, but this was our starting pressure. We then heated the sample chamber to 250°C and the HF filter to 375°C.

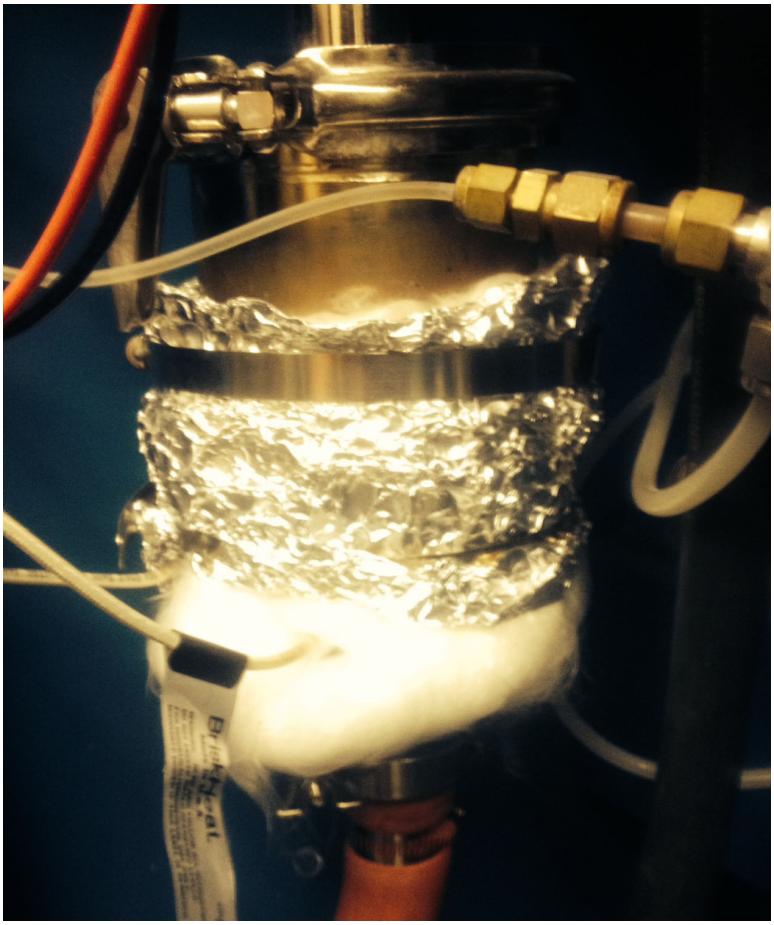

Figure 2.5 A picture of the HF trap we placed between the sample chamber and roughing pump.This was filled with steel wool and aluminum shavings to help diffuse the HF gas before it reached the pump.

These were measured by a thermocouple inside the sample chamber and a voltmeter attached to two leads on the outside of the filter chamber. We also started to flow H_2 into the bypass valve and ignited it into plasma using the microwave generator. Sometimes the generator itself was not able to ignite the plasma and we used a handheld tesla coil to ignite the plasma. Once the chambers had reached our desired temperatures we began the deposition process.

The deposition process is a multistep process as outlined in section 1.3 of the introduction. The first step is to open the source valve on the WF_6 container to fill a limited section of the steel line with WF_6 gas. After waiting a specified amount of time for the gas to disperse in the line we closed the source valve and opened the sample chamber valve to allow the WF_6 gas to disperse. This was so that we could control the amount of gas being used for each flow cycle. After closing the chamber and allowing the gas to deposit onto the carbon nanotubes we redirected the hydrogen plasma from a bypass valve to go straight into the sample chamber. The plasma was flowed through the chamber for a set amount of time to break off fluorine from the WF_6 molecules and allowing more nucleation sites for additional WF_6 deposition on the next cycle. The plasma was then diverted back to the bypass valve and the chamber was pumped down to vacuum again. This cycle was then repeated multiple times to achieve noticeable deposition. After putting in our parameters, the Labview program controlled the whole deposition. We input flow rates, flow times for each gas, wait times, and the desired number of cycles and then let the program run the system. Once the run was over we ended the H_2 flow and purged the system of WF_6 using argon. We shut off power to the heaters, turned on a cooling fan, and then waited for the sample chamber to reach 50°C. After that we removed the samples and used a Scanning Electron Microscope (SEM) with Energy Dispersive X-ray Spectroscopy (EDS) capability to do qualitative measurements of our deposition.

Chapter 3

Discussion

3.1 Pressure and Temperature Controls

Our main objective of this project was to create high-density tungsten microstructures, avoiding problems with capping and allowing for a deeper penetration of our metal into the carbon nanotube forest. To aid penetration we tried to increase the mean free path of molecules inside our sample chamber. The formula for mean free path is as follows:

$$\lambda = \frac{RT}{\sqrt{2}\pi d^2 N_A P} \tag{3.1}$$

To increase the λ value we decreased pressure (P) with our roughing pump to approximately 4 millitorr and increased temperature (T) values in the sample chamber. This prevented obstructions for the WF_6 molecules so that they had a better chance of reaching the inside of the sample.

3.2 SEM and EDAX Analysis

3.2.1 Initial Runs

Our initial runs had very limited deposition. We were unable to obtain a hydrogen plasma for these runs, so the WF_6 was combined with the less-reactive H_2. We kept the chamber at 225°C and flowed each gas into the chamber for 30 seconds with a wait time of 5 seconds in between gases. We performed 8 cycles. Figure 3.1 shows the EDS measurements of a section of the top of our nanotube forest. The final sample was measured to be only 17% tungsten. As we were hoping for a high density tungsten structure, we next focused on achieving ignition of a hydrogen plasma to improve WF_6 HF reactions.

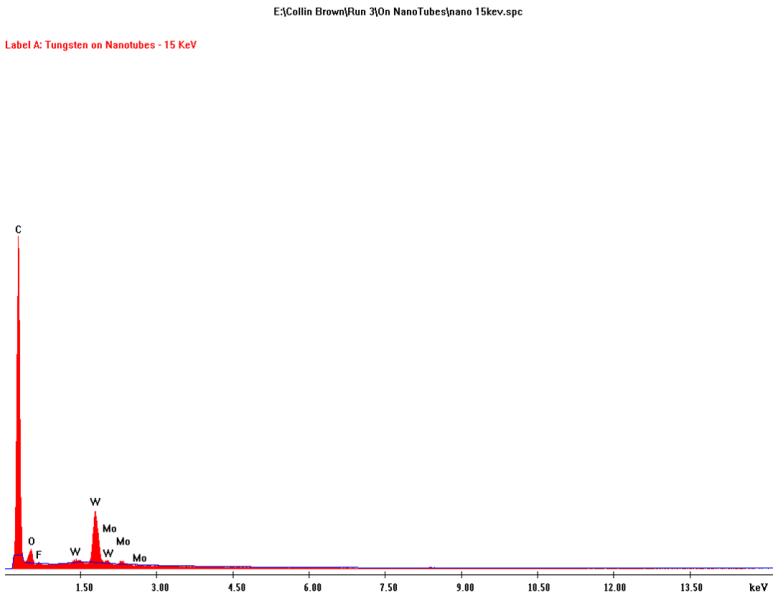

Figure 3.1 The EDS measurements for the initial run. Chemical composition was measured to be 76% carbon and 17% tungsten.

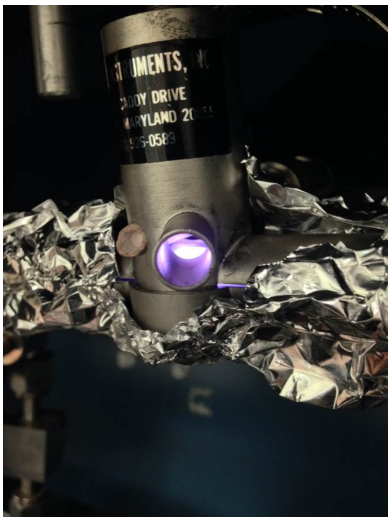

Figure 3.2 A view of the hydrogen plasma being created inside the microwave generator antenna.

3.2.2 Incorporating the Hydrogen Plasma

We were able to ignite the plasma with a handheld tesla coil. The sample chamber was 220°C and we shortened exposure times of both reactants to 5 seconds. We performed 120 cycles on this particular run and achieved chemical measurements of 60% carbon and 23% tungsten. The change from H_2 to a hydrogen plasma increased deposition of our samples from 17% to 23%, but this was still not significant deposition. The remaining percentages in our samples were traces of fluorine and silicon. Our next step was to try ozone treatment of the nanotube forests before deposition.

3.2.3 Incorporating Ozone Treatment

We exposed our nanotube forests to ozone treatment before deposition, creating more nucleation sites on the nanotube walls. The intent was to increase WF_6 deposition on the tubes, and also has the added benefit of increasing the electrical conductivity of the nanotubes themselves [6]. After incorporating ozone treatment into our process we saw the percentage of tungsten in our structure increase from 23% to 68% coating on the outside of the CNT forest. This was a significant amount

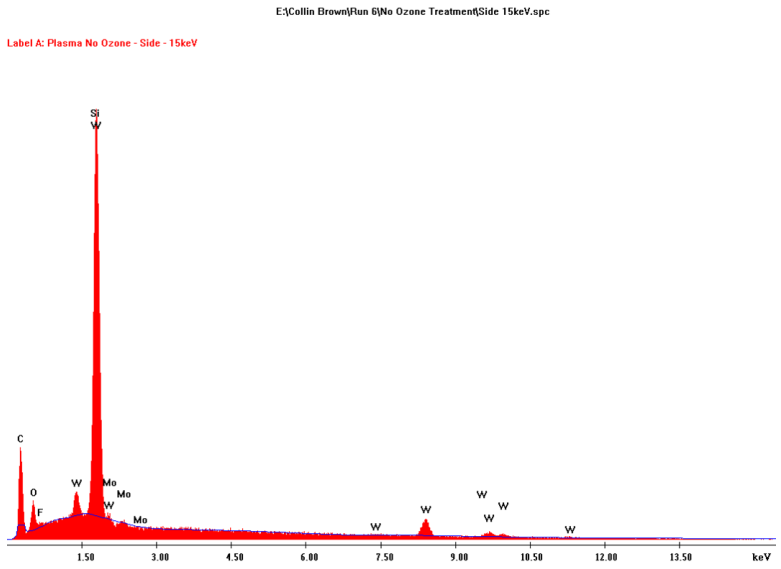

Figure 3.3 The EDS measurements for a run using plasma. Chemical composition was measured to be 60% carbon and 23% tungsten.

of deposition on our nanotube forests, as shown by Figure 3.4. We were pleased to see this amount of deposition on the outside structure, and next investigated the depth of infiltration of tungsten.

3.3 Uniformity of Deposition

In order to approximate how uniform our deposition was, we scraped away the outside layer of a tungsten-coated structure. We were able to position the sample in the SEM in order to get a view of the structure from the side, whereas all our previous measurements had been top down views of the sample. We saw a noticeably decreasing density of tungsten as the scan moved deeper into the forest towards the silicon base. Figure 3.5 shows the limited deposition found inside the structure, and subsequent scans showed less tungsten particles as the target area moved down.

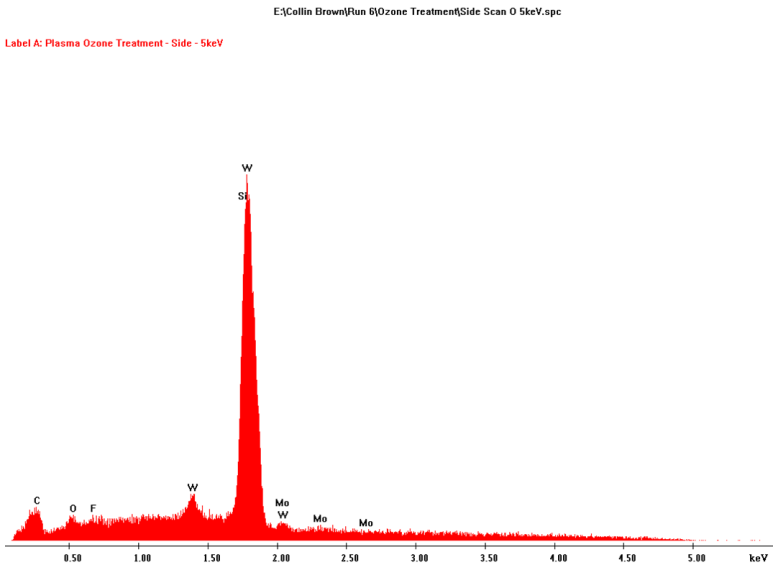

Figure 3.4 The EDS measurements for a run using plasma combined with ozone treatment. Chemical composition was measured to be 12% carbon and 68% tungsten.

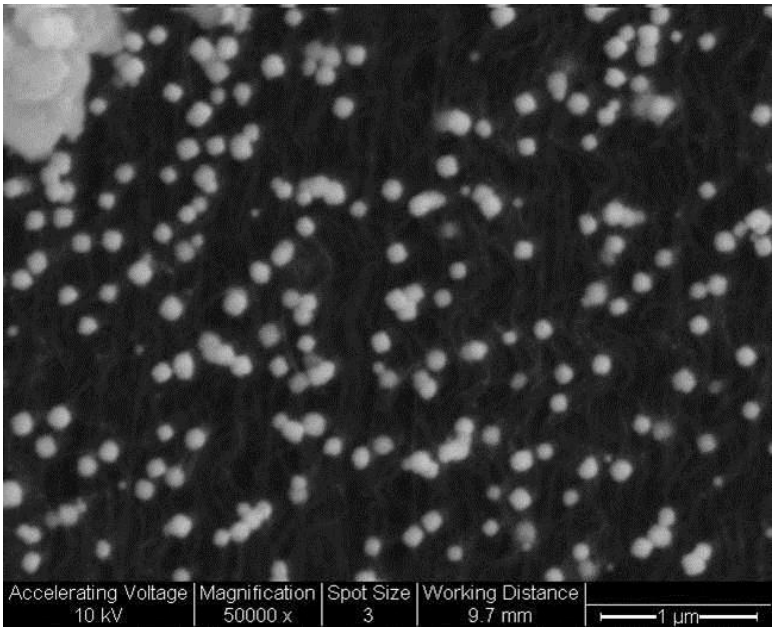

Figure 3.5 This is a cross-sectional view of tungsten deposits in the inner forest.

3.4 Mechanical and Electrical Characterization

After achieving deposition, we attempted to characterize our tungsten structures by measuring electrical resistivity and mechanical flexibility. In order to perform these tests we needed to remove the structures from the substrate using the "liftoff" process. This involved soaking the sample wafer in a potassium hydroxide (KOH) bath, which would etch away the top layer of silicon from the wafer. This would leave free standing structures that could then be analyzed. During "liftoff", however, the structures broke apart due to limited deposition and could not be used for any analysis.

3.5 Conclusion

We were able to achieve tungsten deposition on the carbon nanotube forests, as evidenced by the SEM images in Figure 3.6 where we can see the crystal structures of body-centered cubic tungsten. This gave credibility to our EDS measurements which showed tungsten deposition on the outside surface of the structure. We determined that the best deposition occurred when the samples had been ozone treated before deposition and when we submitted the samples to upwards of 120 cycles of alternating WF_6 and hydrogen plasma exposure. This was able to give us an outside chemical structure composition of 68% tungsten. This deposition, however, did not penetrate well to the inner areas of the nanotube forest. We were unable to achieve mechanical and electrical characterizations of our structures because of limited deposition.

The next step of this project is to continue adjustment of the deposition process. More uniform deposition could be achieved through adjustment of temperature, cycle number, flow rates, exposure time, and wait time between gases. Better deposition would create a more solid structure that could be released from the substrate and allow for analysis of physical properties.

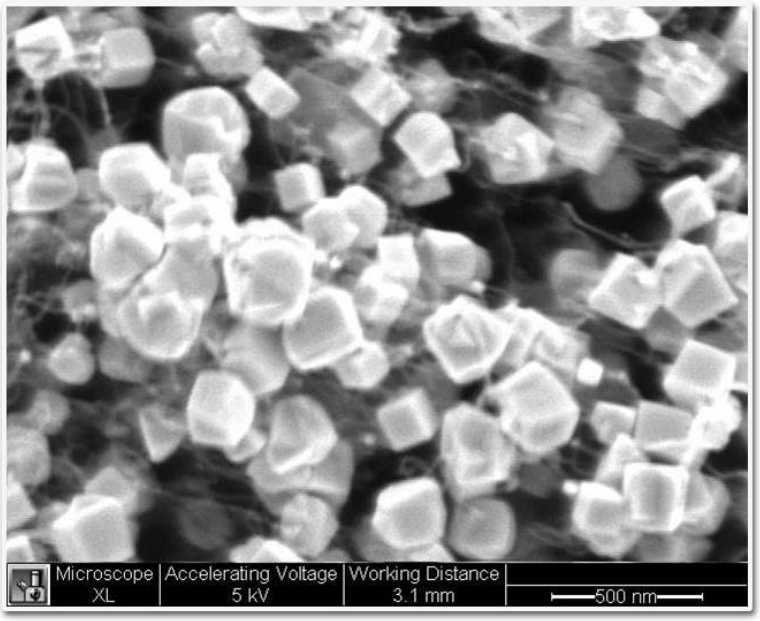

Figure 3.6 EDS measurements of these crystals show no difference between bright and dark spots. The cubic structures seen in this image are a good indicator of achieving BCC tungsten.

Bibliography

[1] J. Xie, Y. Hao, Q. Shen, H. Chang, and W. Yuan, "A dicing-free SOI process for MEMS devices based on the lag effect," Journal of Micromechanics and Microengineering **23,** 125033 (2013).

[2] R. Hansen, *Mechanical and Electrical Properties of Carbon-Nanotube-Templated Metallic Microstructures* (Brigham Young University Department of Physics and Astronomy, 2012).

[3] K. Moulton, N. Morrill, A. Konneker, B. Jensen, R. Vanfleet, D. Allred, and R. Davis, "Effect of iron catalyst thickness on vertically aligned carbon nanotube forest straightness for cnt-mems," Journal of Micromechanics and Microengineering **22,** 55004–55012 (2012).

[4] D. M. McKenna, *Tungsten Infiltrated Carbon Nanotube Forests As A Framework For 3-D Microfabrication* (Brigham Young University Department of Physics and Astronomy, 2011).

[5] D. N. Hutchison, *Vertically Aligned Carbon Nanotubes as a Framework for Microfabrication of High Aspect Ratio MEMS* (Brigham Young University Department of Physics and Astronomy, 2008).

[6] E. Najafi, J. Kim, S. Han, and K. Shin, "UV-ozone treatment of multi-walled carbon nanotubes for enhanced organic solvent dispersion," Colloids and Surfaces A: Physicochemical and Engineering Aspects **284,** 373–378 (2006).

Index